Available online at www.sciencedirect.com
ScienceDirect
Geochimica et Cosmochimica Acta 73 (2009) 5959–5974
Geochimica et Cosmochimica Acta
www.elsevier.com/locate/gca

Ultra-low rare earth element content in accreted ice from sub-glacial Lake Vostok, Antarctica

Paolo Gabrielli [a,b,*], Frederic Planchon [a,1], Carlo Barbante [a,c], Claude F. Boutron [d], Jean Robert Petit [d], Sergey Bulat [d,e], Sungmin Hong [f], Giulio Cozzi [c], Paolo Cescon [a,c]

[a] Institute for the Dynamics of Environmental Processes-CNR, University of Venice, Ca'Foscari, 30123 Venice, Italy
[b] School of Earth Sciences and Byrd Polar Research Center, The Ohio State University, Columbus, OH 43210, USA
[c] Department of Environmental Sciences, University of Venice, Ca'Foscari, 30123 Venice, Italy
[d] Laboratoire de Glaciologie et Géophysique de l'Environnement (UMR 5183 Université Joseph Fourier de Grenoble/CNRS), 38402 St. Martin d'Heres cedex, France
[e] Division of Molecular and Radiation Biophysics, Petersburg Nuclear Physics Institute, RAS, Leningrad region, 188300 Gatchina, Russia
[f] Korea Polar Research Institute, 7-50, Songdo-dong, Yeonsu-gu, Incheon 406-840, South Korea

Received 14 November 2008; accepted in revised form 18 May 2009; available online 28 May 2009

Abstract

This paper reports the first rare earth element (REE) concentrations in accreted ice refrozen from sub-glacial Lake Vostok (East Antarctica). REE were determined in various sections of the Vostok ice core in order to geochemically characterize its impurities. Samples were obtained from accreted ice and, for comparison, from the upper glacier ice of atmospheric origin (undisturbed, disturbed and glacial flour ice). REE concentrations ranged between 0.8–56 pg g^{-1} for Ce and 0.0035–0.24 pg g^{-1} for Lu in glacier ice, and between <0.1–24 pg g^{-1} for Ce and <0.0004–0.02 pg g^{-1} for Lu in accreted ice. Interestingly, the REE concentrations in the upper accreted ice (AC_1; characterized by visible aggregates containing a mixture of very fine terrigenous particles) and in the deeper accreted ice (AC_2; characterized by transparent ice) are lower than those in fresh water and seawater, respectively. We suggest that such ultra-low concentrations are unlikely to be representative of the real REE content in Lake Vostok, but instead may reflect phase exclusion processes occurring at the ice/water interface during refreezing. In particular, the uneven spatial distribution (on the order of a few cm) and the large range of REE concentrations observed in AC_1 are consistent with the occurrence/absence of the aggregates in adjacent ice, and point to the presence of solid-phase concentration/exclusion processes occurring within separate pockets of frazil ice during AC_1 formation. Interestingly, if the LREE enrichment found in AC_1 was not produced by chemical fractionation occurring in Lake Vostok water, this may reflect a contribution of bedrock material, possibly in combination with aeolian dust released into the lake by melting of the glacier ice. Collectively, this valuable information provides new insight into the accreted ice formation processes, the bedrock geology of East Antarctica as well as the water chemistry and circulation of Lake Vostok.
Published by Elsevier Ltd.

1. INTRODUCTION

Lake Vostok is the largest of more than 145 sub-glacial lakes discovered beneath the East Antarctic ice sheet (Siegert et al., 2005). This large reservoir of freshwater (Kapitsa et al., 1996) is maintained in the liquid state by a positive heat balance at one end of the lake where the overlying ice is thicker and the pressure melting point consequently lower (Petit et al., 2005). Notably, Lake Vostok

* Corresponding author. Address: School of Earth Sciences and Byrd Polar Research Center, The Ohio State University, Columbus, OH 43210, USA. Fax: +1 614 2924697.
E-mail address: gabrielli.1@osu.edu (P. Gabrielli).
[1] Present address: The Royal Museum for Central Africa, Geology Department, 3080 Tervuren, Belgium.

0016-7037/$ - see front matter Published by Elsevier Ltd.
doi:10.1016/j.gca.2009.05.050

might constitute a long-standing isolated ecosystem, possibly supporting ancient microbial organisms (e.g. Christner et al., 2006; Lavire et al., 2006).

Lake Vostok measures approximately 275 by 65 km and has a total area and volume of 15,500 km^2 and ~6100 km^3, respectively (Masolov et al., 2008). The water depth reaches a maximum of 1650 m in the south and 150 m in the north while the overlying ice thickness varies between 3750 m in the south and 4150 m in the north. The ice ceiling is thus tilted and lies 250 and 750 m below sea level at the southern and northern ends of the lake, respectively (Masolov et al., 2001). Ice is actively accreted to this ceiling in the southern part of the lake whereas melting occurs in the northern portion (Siegert et al., 2001). Exactly how this accretion is accommodated remains unclear. Stable isotopes suggest that accreted ice could originate from a complex freezing process involving a slush of frazil ice, generated in supercooled water, and its host water which is subsequently frozen in separate pockets (Jouzel et al., 1999). However, the stable isotopic values could also be explained by the glacier melting process (Souchez et al., 2003).

The age and the origin of Lake Vostok's water remain uncertain. One possibility is that this large freshwater reservoir originates directly from melting of the overlying ice sheet (Siegert et al., 2000; Studinger et al., 2004). Recently, the suggestion that different Antarctic sub-glacial lakes are interconnected, with channels transferring their water from one reservoir to another (Wingham et al., 2006), has provided a dynamic view of their sub-glacial biotic and physical–chemical processes. However, as Lake Vostok is remote from the other Antarctic sub-glacial lakes, this basin could have been confined for millions of years, possibly since the onset of Antarctic glaciation.

An impetus for the study of Lake Vostok came from an international ice sheet deep drilling program conducted above the southern margin of Lake Vostok, where ice accretion occurs (Fig. 1). The ice core retrieved is the deepest ever obtained and its upper part, down to a depth of 3310 m, revealed climatic history and atmospheric composition over the last four glacial cycles (Petit et al., 1999). Below 3310 m depth, ice can be subdivided into three sections. Ice at depths between 3310 and 3450 m (disturbed ice) is of atmospheric origin but does not offer interpretable paleoclimate data due to strain by ice flow upstream of the drilling site. Ice between 3450 and 3538 m (glacial flour ice) is similar to disturbed ice except that it contains entrained basal material due to contact with the bedrock (Simoes et al., 2002; Souchez et al., 2002). In contrast, ice below 3538 m originates from the refreezing of Lake Vostok water (accreted ice) (Jouzel et al., 1999). Drilling operations stopped at 3659 m in the 2006–2007 season, just ~100 m above the ice/water contact (Fig. 1).

The accreted ice can be further subdivided into two types. Accreted ice between 3538 and 3609 m, (hereafter Accreted Ice Type I; AC_1) is mainly characterized by a number of visible inclusions (up to few millimeters in size) suggested to be remnants of surface and/or hydrothermally-flushed out bedrock (deep vent) material (Jouzel et al., 1999; Bulat et al., 2004; Delmonte et al., 2004b). Interestingly, most of these inclusions vanish when the ice is melted (De Angelis et al., 2004) indicating that they are soft aggregates of very fine particles (De Angelis et al., 2005). However, two visible solid clasts of fine-grained lithic material were also found in AC_1 (Leitchenkov et al., 2007). In contrast with AC_1, the lower 50 m (3609–3659 m), (hereafter Accreted Ice Type II; AC_2) is characterized by the lack of visible inclusions. This difference is likely due to AC_1 and AC_2 originating from lake water that accreted in a shallow embayment (where the inclusions were entrapped) and over the deep water in the southwestern part of the lake, respectively (Bell et al., 2002; De Angelis et al., 2004) (Fig. 1).

Although Lake Vostok water has not been sampled directly, the deepest sections of the accreted ice have provided preliminary information on the physical, chemical and biological properties of this large sub-glacial reservoir. In addition to variation in the number of visible aggregates, the δD, gas content, crystal size, electrical conductivity (Jouzel et al., 1999) and the ionic content (De Angelis et al., 2004) all change abruptly at the glacier ice/accreted ice transition.

Very few investigations have been conducted in order to explain the origin of impurities entrapped in AC_1 (De Angelis et al., 2004, 2005; Leitchenkov et al., 2007). As a whole, scattered aggregates investigated by in situ X-ray fluorescence (De Angelis et al., 2005) appear to be composed of a mixture of fine aluminosilicate particles, carbonate-rich particles (5–10 μm) and larger structures where sulfate is linked to Mg (De Angelis et al., 2005). They also contain significant amounts of calcium sulfate (De Angelis et al., 2004), reduced sulfur species, Si (also in other minerals besides aluminosilicates) and to a lesser extent, O, P and Na. A different mineralogical analysis pointed out that these soft aggregates consist mainly of clay–mica minerals (possibly illite and chlorite; less than 0.5 μm in size; 30–60% of the total mineral content), subangular to angular quartz grains (10–40 μm; 30–60%) and a variety of accessory minerals (Leitchenkov et al., 2007).

In contrast with other species, Cl^- and Na^+ were found to be homogeneously distributed as NaCl throughout large individual crystals of accreted ice (De Angelis et al., 2004). This finding was confirmed by the in situ observation of numerous fine (3–10 μm) diffused liquid brine micro-droplets coexisting with the sparser and larger aggregates. The X-ray signal from these droplets is dominated by Cl and significant amounts of Na (De Angelis et al., 2005). Altogether these observations were interpreted as evidence of haline water pulses carrying fine, solid debris from a deeper, evaporitic reservoir into the lake and of the presence of hydrothermal activity at the lake bottom (De Angelis et al., 2004, 2005). Hydrothermal input to the lake, related to tectonic activity, would also explain bacterial DNA fragments discovered in the accreted ice (Bulat et al., 2004; Lavire et al., 2006).

Rare earth elements (REE) have been widely adopted as proxies for several geochemical processes in cosmochemistry, igneous petrology, sedimentology and oceanography. This is because REE have a relative immobility in the terrestrial crust and a low solubility during weathering, but are readily fractionated in the environment because of their characteristic radius contraction across the lanthanide series (Henderson, 1984). As they are mostly transported in the

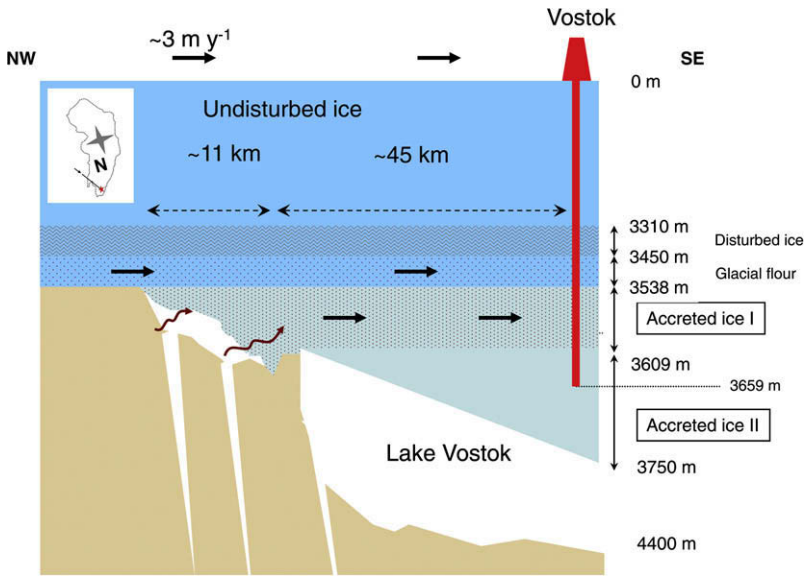

Fig. 1. Sketch (not to scale) of the ice sheet and Lake Vostok along the ice flow line (noted with black arrows in the main figure and insert). The ice sheet flows from over the NW end of the lake to the SE. The lower disturbed ice is strained by the ice flow upstream of the drilling site. Glacial flour ice is similar to disturbed ice except that it contains entrained basal material due to contact with the bedrock. The presence of visible aggregates in accreted ice I is likely related to its formation in the shallow, NW end of the lake. Accreted ice II forms in the deeper, SE end and lacks such aggregates. Faulting of the basement allows water to penetrate deeply into the bedrock. Figure is adapted from Bulat et al. (2004).

particulate phase, the REE content of particulate matter is generally characteristic of the original source (Henderson, 1984). REE are thus a useful tool for the geochemical characterization of the impurities entrapped in the Vostok ice core.

Here we present REE concentrations determined in various sections of the Vostok ice core originating both from glacier and accreted ice. Only a few accreted ice sections were made available for this study and an additional contingent limitation is that, as Lake Vostok has not been sampled yet, we cannot directly compare the REE composition of the water and of the ice. Another difficulty inherent to our study involves the identification of the respective REE insoluble/soluble contributions to accreted ice from Lake Vostok (bedrock particles and dissolved ions) and melted glacier ice (aeolian particles). However, comparison of REE concentrations, Ce anomalies and normalized crustal REE patterns in glacier ice and accreted ice may provide the first indirect information regarding the insoluble particles/soluble species that are suspended/dissolved in Lake Vostok water.

Interestingly, REE determination in glacier ice also has the potential to provide information about the sources of aeolian dust reaching the Antarctic ice sheet during past climatic cycles, in similar fashion to using Sr and Nd isotopes (Delmonte et al., 2004a), and about detritus from the East Antarctic geologic basement entrapped in the glacial flour ice (Simoes et al., 2002).

2. EXPERIMENTAL

2.1. Sample description

The 3659 m Vostok ice core was drilled from a fluid-filled (kerosene–forane) hole at the Russian Vostok Station (78°28′S, 106°48′E; 3488 m; mean annual surface temperature −55 °C) in East Antarctica. Nineteen glacier ice sections were available from the upper part of the core (127–2751 m) covering the Holocene and extending through the last two glacial cycles back to ~237 kyr BP (Marine Isotopic Stage (MIS) 7.5) (Hong et al., 2004; Gabrielli et al., 2005). Seventeen additional sections (length 35–45 cm, diameter 10 cm) were available from the deepest part of the Vostok core (3271–3659 m). Among those, two sections were from the deepest, undisturbed ice layers (3271 and 3294 m) corresponding to MIS 11 (~400 kyr BP), three sections were from the disturbed ice (3348, 3374 and 3398 m) and three were from the glacial flour ice (3473, 3500 and 3523 m). Four ice sections were part of AC_1, the upper two of which (3556 and 3578 m) showed several visible soft inclusions while the lower two (3593 and 3609 m) were characterized by clear ice. Although the section at 3609 m was at the boundary between AC_1 and AC_2, it was assigned to AC_1 based on the occurrence of several visible inclusions in the adjacent ice upcore and REE ratios consistent with the other three AC_1 sections (see below). The five deepest sections (3613, 3621, 3635, 3650 and 3659 m) were part of AC_2.

2.2. Sample preparation

An accurate determination of trace elements in the Vostok ice core is analytically challenging due to their extremely low concentrations and the consequent high risk of contamination (Gabrielli et al., 2005, 2006b; Hong et al., 2005). Extremely clean procedures and highly sensitive instrumental techniques were thus required. Depending on the section length, various inner- and outer-core samples

were obtained by chiseling several external layers under ultra-clean conditions (Candelone et al., 1994; Gabrielli et al., 2004). One or more aliquots per ice layer were obtained after melting each inner or outer sample in a 1 L low-density polyethylene bottle (LDPE; Nalgene) under a class 100 clean bench.

A total of 106 aliquots (Electronic annex 1) were obtained from the Vostok ice sections. Of those, 28 were from the four AC_1 sections and 13 were from the five AC_2 ice sections. However, these latter five sections originated from another project and were decontaminated using a different procedure (Bulat et al., 2008). In this case, each ice section was cut into three samples that were transferred to a Cryo-Box, cooled at −15 °C and exposed to clean room temperature for about 20 min. Next, each ice section was inserted into a 1-L glass beaker, treated with Biohit Proline Biocontrol spray and then briefly immersed in another 1-L glass beaker filled with 0.5 L of ultra-pure water (Elga system). The water was then discharged and the ice section rinsed with ultra-pure water. The ice was then transferred to an ultra-clean 125 mL large-mouth LDPE bottle, sealed in three polyethylene bags and kept frozen until the analysis. Handling was performed using Class 1000 vinyl gloves. Although concentrations in these five sections are generally the lowest observed in the entire study, we believe that the reagents and materials used (which are unconventional for trace element analysis) might have introduced a very slight contamination, especially for the most abundant REE such as La, Ce, Pr and Nd. However, as we cannot exclude these data as unreliable, we prudently assume that these ultra-low REE concentrations lie at the upper limit of the genuine values. Accordingly, we do not emphasize REE ratios obtained from these five sections in the following discussion.

2.3. Analysis

Samples were analyzed using an ultra-sensitive method specific to the determination of REE by Inductively Coupled Plasma Sector Field Mass Spectrometry (ICP SFMS) in polar ice. This method, extensively illustrated elsewhere (Gabrielli et al., 2006a), is based on ICP SFMS coupled with a micro-flow nebulizer and a desolvation system. With this setup REE determination can be performed down to the sub-pg g^{-1} level (1 pg $g^{-1} = 10^{-12}$ g g^{-1}) in ~1 ml of sample acidified to pH = 1 with HNO_3 (ultra-pure grade).

The use of the desolvation system greatly reduced spectral interferences from oxide formation. Any interfering contributions not removed by the desolvation system, were quantified and subtracted whenever necessary. During these analyses, however, an interference affected the Gd concentrations and it was not possible to perform a reliable quantification and mathematical subtraction of the false positive counts per second. The Gd values are therefore reported only as upper limits of the genuine concentrations.

A matched calibration curve method was used for the quantification of the analytes. Instrumental detection limits ranged from 0.0004 pg g^{-1} for Lu to 0.03 pg g^{-1} for Gd. The precision, in terms of relative standard deviation on 10 replicates, ranged from 2% for La, Ce, Pr and Lu, up to 10% for Er, Tm and Yb. To estimate the accuracy, we carried out a recovery test by adding standard spikes of a REE multi-element stock solution to a real sample. The REE concentrations measured in a sample spiked with 0.62 pg g^{-1} and calculated using the slopes provided by the matched calibration were found to fall between 95% and 105% of the expected value.

We also performed a test on real glacial/interglacial Antarctic ice samples to assess the REE mass fraction determined by our method (1% HNO_3 acidification) when compared to the total REE content obtained by adopting a full acid digestion (Gabrielli et al., 2009). Briefly, the REE mass fraction obtained was ~55% for LREE, ~50% for MREE and ~40% for HREE. This was essentially identical at low (interglacial) and high (glacial) levels; for instance, the Tb fraction determined at high and low concentration levels was ~50% in both cases. This suggests that no methodological REE fractionation due to different concentration levels occurs during sample analysis. Although LREE appears slightly overestimated by our method with respect to MREE and HREE (~9% and ~27%), this is unlikely to explain the much larger LREE enrichments (~50% and ~200%) observed in the REE patterns in AC_1 (see below).

3. RESULTS AND DISCUSSION

3.1. REE distribution within the ice sections

Radial REE concentration profiles were determined by successively analyzing the inner core and adjacent outer layers obtained by chiseling the glacier ice and AC_1 sections (Fig. 2). Because the outermost layer was expected to be heavily contaminated by drilling fluid (Gabrielli et al., 2005), only a few samples were analyzed. These samples did contain much higher REE concentrations (Electronic annex 1) and they are not discussed further.

In general, radial REE concentration profiles of undisturbed ice sections are very different than those from disturbed ice, glacial flour ice and AC_1. In undisturbed ice, REE concentrations show only minor variations between the outer layers and the inner core. These can likely be attributed to analytical uncertainty, indicating that the REE content is homogeneously distributed within the ice section and that contamination has not penetrated into the core. As commonly assumed in these kinds of studies, REE concentrations in the inner cores are considered representative of the genuine REE content at a given depth.

In contrast, most of the disturbed ice, glacial flour ice and AC_1 sections do not exhibit consistent REE concentrations. Rather, they appear to vary randomly in these three types of ice up to a factor of 4, 6 and 24, respectively. This behavior was not observed in any of our previous ice core studies (e.g. Vallelonga et al., 2002a; Gabrielli et al., 2004). It is very unlikely that this variability can be explained by contamination as when this occurs, concentrations are found to steadily decrease from the outermost contaminated layer towards the inner part of the core, in contrast with our findings. In addition, consistent REE normalized crustal patterns of the different REE concentrations between the inner core and external layers of the

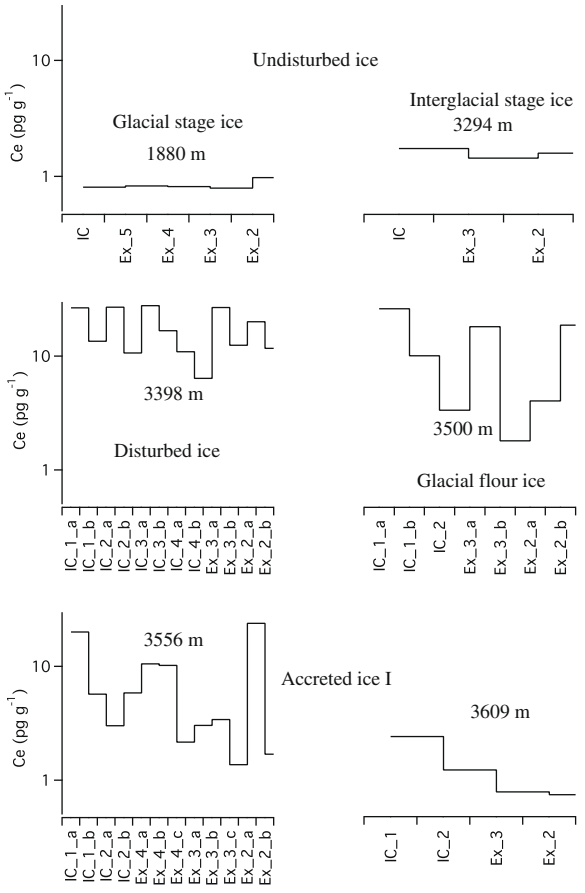

Fig. 2. Profiles of internal and external radial Ce concentrations (log-scale) as examples of REE variability in six sections of the Vostok ice core. Inner cores are labeled with "IC" while numbers indicate consecutive sub-samples along the inner core. External layers are labeled with "Ex" while the numbers shows different radial layers (Ex_1 not shown as it is contaminated; Ex_2...Ex_n). Additional lettering for "IC" and "Ex" indicates multiple aliquots obtained from the same liquid sample. Undisturbed ice (1880 and 3294 m) shows homogeneous concentrations through the ice sections. In contrast, disturbed ice (3398 m) and glacial flour ice (3500 m) show very heterogeneous concentrations. Also, Accreted Ice Type I (3556 and 3609 m) shows heterogeneous concentrations.

same ice sections were found (Fig. 3). If contamination played a role, a significant Eu enrichment with respect to the other normalized REE, as that found (~10) in an obviously contaminated outermost external layer (1880 m; undisturbed glacier ice; Electronic annex 1), might be expected. This was not observed in any of the samples considered supporting the lack of contamination.

As many visible aggregates were observed in AC_1, an inhomogeneous distribution of insoluble particles carrying REE is expected. Support for the particulate nature of REE in AC_1 is provided by their correlation with typical crustal elements such as Al, Mn, Fe, Co, Rb and the lack of correlation with soluble elements such as Ca and Na (see below).

Bedrock particles with a larger mode diameter (3.4 μm) than in the overlying disturbed ice (2.1 μm) and relatively large terrigeneous aggregates up to 30 μm in diameter were detected in the fine grained ice layers of the glacial flour ice (Simoes et al., 2002). Thus the anomalous radial REE profiles observed in two out of three glacial flour ice sections might be explained by the occasional presence of bedrock particles/aggregates. However, heterogeneous REE concentration profiles were also observed in two out of three sections retrieved from the upper disturbed ice (3374 and 3398 m). Until now, no evidence of bedrock particles/aggregates at these depths has been reported. One explanation for these anomalous profiles is that bedrock material is present at shallower depths in the core than previously thought. Alternatively, this REE heterogeneity could be due to cm-scale folds in the ice caused by differential mechanical behavior between ice with high versus low aeolian particle content (Dahl-Jensen et al., 1997).

Further insight into the nature of the REE-carrying particles/aggregates comes from analysis of multiple aliquots of the same melted ice sample (indicated with lettering in Fig. 2). From each sample, if enough volume was available, two to four aliquots were collected in 30 ml LDPE bottles and then acidified with 1% ultra-pure HNO_3 at pH = 1. For disturbed ice, glacial flour ice and AC_1, a surprising variability in REE concentrations was found even for aliquots originating from the same melted ice sample. It is important to note that repeated analyses on the same acidified aliquot resulted in identical REE concentrations. This suggests that a few, relatively large aggregates were heterogeneously distributed in the melted, non-acidified solution and dissolved only after acidification.

We recognize that full acid digestion was an alternative method of sample preparation. We choose to employ simple acidification, however, as a reliable quantification of ultra-low REE concentrations in accreted ice requires excellent blank levels and these were unlikely to be obtained with a full acid digestion. With respect to present limits in state-of-the-art ultra-trace element determination in Antarctic ice, it is likely that our approach is, for the moment, the only feasible strategy.

3.2. REE concentrations

The large heterogeneity observed in the radial REE concentrations makes it difficult to define a representative REE concentration for a given depth in the disturbed ice, glacial flour ice and AC_1 sections. Because the outer layers are as likely to provide genuine REE concentrations as the inner core, we assume that the median REE value of all ice samples from a section is representative of the concentration for a given depth. We also use the median REE concentration of each AC_2 sub-sample, as this provides internal consistency in the statistical analysis of different samples and allows us to account for some REE concentrations below the limit of detection. All the REE main statistics are reported in Tables 1 and 2 while the full data set is reported in Electronic annex 1. For convenience, we define light REE (LREE; La, Ce, Pr, Nd), medium REE (MREE; Sm, Eu, Gd, Tb, Dy, Ho) and heavy REE (HREE; Er, Tm, Yb, Lu).

The logarithm of the typical REE concentrations in each type of ice (calculated as a median of the median sample

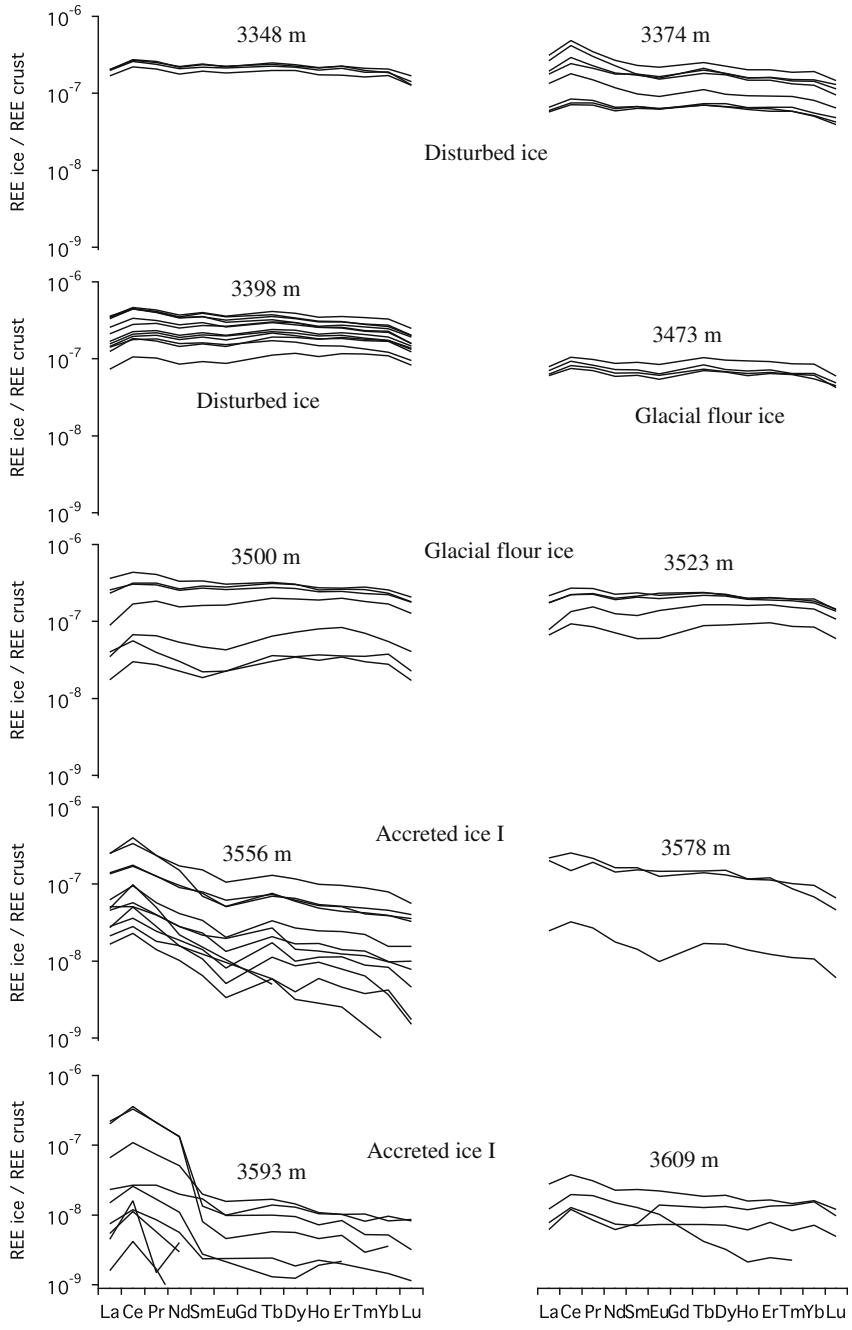

Fig. 3. Logarithm of the crustal normalized REE concentrations (mean crustal values from Wedepohl (1995) in all samples from each ice section retrieved from the Vostok basal ice (excluding Accreted Ice Type II). As Gd is biased by instrumental spectral interferences, its normalized concentration is only graphically interpolated through Eu and Tb. Only samples at 3348 and 3473 m show similar normalized concentrations. In contrast, samples from the other sections show different REE concentrations indicating an inhomogeneous distribution of REE within the ice. However, generally similar REE patterns within the same ice section support a homogeneous REE composition and indicate that drilling fluid (likely enriched in Eu, see text) has not penetrated into the core. We also note that, REE patterns from the undisturbed, disturbed and glacial flour ice sections are similar. However, a light REE (LREE) enrichment is observed in a few samples from disturbed ice (3374 and 3500 m). LREE enriched patterns are clearly observed in the Accreted Ice Type I samples.

concentrations), produces the well known REE seesaw pattern caused by the alternation of high and low abundances (not shown). As concentrations for all the REE show nearly identical relative variations along the ice depth, we use Ce and Lu (the most and the least abundant REE, respectively) variations as representative examples of the concentration ranges. Concentrations span at least four orders of magnitude (Ce = 56 pg g^{-1} for glacial stage ice; Lu < 0.001 pg g^{-1}, AC_1 and AC_2). The highest REE median concentrations are found in glacial stage ice (Ce = 25 pg g^{-1}; Lu = 0.11 pg g^{-1}) and the lowest are observed in AC_2, (Ce < 0.3 pg g^{-1}; Lu < 0.001 pg g^{-1}). In Fig. 4, Ce is reported as an example

Table 1
REE concentrations (pg gg^{-1}) in the Vostok ice core.

Depth (m)	Type of ice	Value	La	Ce	Pr	Nd	Sm	Eu	Gd	Tb	Dy	Ho	Er	Tm	Yb	Lu
127	Interglacial stage	Inner core	0.6	1.4	0.14	0.36	0.1	0.023	0.11	0.007	0.05	0.010	0.02	0.005	0.03	0.003
150	Interglacial stage	Inner core	0.7	1.9	0.18	0.7	0.18	0.04	0.23	0.018	0.11	0.02	0.05	0.009	0.05	0.006
194	Interglacial stage	Inner core	1.0	3	0.3	0.9	0.22	0.05	0.3	0.03	0.15	0.027	0.08	0.011	0.08	0.009
513	Glacial stage	Inner core	10	24	2.8	10	2.3	0.5	3.0	0.28	1.6	0.3	0.8	0.12	0.8	0.10
938	Glacial stage	Inner core	22	53	6	23	5	1.1	7	0.7	3.6	0.7	1.8	0.25	1.6	0.23
1206	Glacial stage	Inner core	2.4	5	0.6	2	0.5	0.09	0.6	0.05	0.3	0.05	0.12	0.016	0.09	0.015
1514	Glacial stage	Inner core	10	21	2.5	9	1.9	0.4	2.5	0.26	1.5	0.28	0.8	0.11	0.63	0.08
1815	Interglacial stage	Inner core	1.0	2	0.3	1.0	0.3	0.06	0.3	0.03	0.16	0.03	0.08	0.012	0.08	0.011
1880	Interglacial stage	Inner core	0.3	0.8	0.09	0.32	0.11	0.02	0.12	0.011	0.067	0.012	0.04	0.007	0.04	0.005
1917	Interglacial stage	Inner core	3	7	0.8	3	0.7	0.17	1.0	0.10	0.5	0.10	0.27	0.04	0.3	0.04
1999	Glacial stage	Inner core	23	56	7	25	6	1.2	7	0.7	4.1	0.8	2.1	0.30	1.9	0.24
2079	Glacial stage	Inner core	11	25	3.0	11	2.6	0.5	3	0.4	1.8	0.34	0.9	0.13	0.8	0.11
2199	Glacial stage	Inner core	17	40	5	17	3.7	0.8	5	0.4	2.3	0.4	1.1	0.15	1.0	0.12
2378	Glacial stage	Inner core	12	29	3	13	3	0.6	4	0.4	1.9	0.3	1.0	0.13	0.9	0.11
2505	Glacial stage	Inner core	0.7	1.6	0.18	0.6	0.16	0.04	0.2	0.018	0.10	0.018	0.05	0.009	0.05	0.008
2534	Interglacial stage	Inner core	1.9	5	0.5	1.7	0.4	0.09	0.6	0.05	0.3	0.05	0.16	0.02	0.14	0.018
2616	Interglacial stage	Inner core	1.3	3.0	0.33	1.2	0.28	0.06	0.3	0.033	0.15	0.032	0.1	0.011	0.07	0.01
2682	Glacial stage	Inner core	1.8	4.2	0.5	1.7	0.41	0.09	0.55	0.051	0.28	0.06	0.17	0.023	0.14	0.021
2751	Interglacial stage	Inner core	1.6	4	0.4	1.5	0.4	0.08	0.5	0.04	0.21	0.04	0.11	0.015	0.10	0.02
3271	Interglacial stage	Median	1.3	3.4	0.31	1.0	0.18	0.04	0.1	0.019	0.12	0.022	0.06	0.008	0.05	0.005
3294	Interglacial stage	Inner core	0.7	1.8	0.17	0.54	0.09	0.021	0.05	0.012	0.08	0.015	0.04	0.006	0.04	0.004
3348	Disturbed	Median	6	16	1.6	5.8	1.2	0.28	1.1	0.15	0.8	0.17	0.5	0.058	0.38	0.047
3374	Disturbed	Median	3.9	11	1.0	3.3	0.64	0.15	0.6	0.09	0.48	0.09	0.24	0.031	0.20	0.029
3398	Disturbed	Median	7.4	19.2	2.0	7.0	1.42	0.31	1.3	0.18	0.98	0.19	0.50	0.065	0.42	0.054
3473	Glacial flour	Median	2.0	5.3	0.5	1.9	0.36	0.08	0.3	0.05	0.27	0.053	0.15	0.019	0.13	0.016
3500	Glacial flour	Median	4.1	11	1.2	4.0	0.8	0.20	0.7	0.11	0.64	0.13	0.33	0.046	0.28	0.039
3523	Glacial flour	Median	4.2	11	1.3	4.4	0.9	0.24	0.8	0.13	0.7	0.14	0.39	0.05	0.33	0.044
3556	Accreted I	Median	4.0	10	0.8	2.3	0.21	0.04	0.22	0.03	0.13	0.023	0.05	0.007	0.04	0.006
3578	Accreted I	Median	6.0	9	1.29	3.9	0.8	0.16	0.7	0.09	0.50	0.09	0.24	0.026	0.14	0.016
3593	Accreted I	Median	0.7	1.6	0.18	0.54	0.05	0.01	0.06	0.004	0.021	0.004	0.011	0.001	0.007	0.001
3609	Accreted I	Median	0.30	1.0	0.10	0.30	0.05	0.016	0.05	0.007	0.039	0.007	0.022	0.003	0.023	0.003
3613	Accreted II	Median	0.08	0.19	0.01	0.02	<0.01	<0.03	<0.03	<0.002	<0.003	<0.001	<0.002	<0.001	<0.002	<0.001
3621	Accreted II	Median	0.16	0.42	0.06	0.11	<0.01	<0.03	<0.03	<0.002	<0.003	<0.001	<0.002	<0.001	<0.002	<0.001
3635	Accreted II	Median	0.11	0.29	0.01	0.04	<0.01	<0.03	<0.03	<0.002	<0.003	<0.001	<0.002	<0.001	<0.002	<0.001
3650	Accreted II	Median	0.10	0.24	0.04	0.12	<0.01	<0.03	<0.03	<0.002	<0.003	<0.001	<0.002	<0.001	<0.002	<0.001
3659	Accreted II	Inner core	0.13	0.3	0.017	0.07	<0.01	<0.03	<0.03	<0.002	<0.003	<0.001	<0.002	<0.001	<0.002	<0.001

Underscored values are upper limits of concentration.
Concentrations below the limit of detection (LOD) are reported as <LOD.

Table 2
Main statistics for the REE in the different types of ice.

Statistic	Type of ice	La	Ce	Pr	Nd	Sm	Eu	Gd	Tb	Dy	Ho	Er	Tm	Yb	Lu
Median (pg g^{-1})	Interglacial stage	1.2	2.8	0.29	1.0	0.24	0.05	<0.3	0.03	0.15	0.03	0.08	0.011	0.08	0.010
	Glacial stage	11	25	3.0	11	2.6	0.5	<3.5	0.35	1.8	0.34	0.9	0.13	0.8	0.11
	Disturbed	6.0	16	1.6	5.8	1.2	0.3	<1.1	0.15	0.8	0.17	0.46	0.06	0.38	0.05
	Glacial flour	4.1	11	1.2	4.0	0.8	0.2	<0.7	0.11	0.6	0.13	0.33	0.046	0.28	0.04
	Accreted I	2.4	5.3	0.5	1.4	0.13	0.026	<0.14	0.02	0.08	0.02	0.04	0.005	0.03	0.004
	Accreted II	<0.1	<0.3	<0.02	<0.07	<0.01	<0.03	<0.03	<0.002	<0.003	<0.001	<0.002	<0.001	<0.002	<0.001
Median ratios	Glacial/Interglacial	9	9	10	11	11	10	_	13	12	12	11	12	10	11
	Glacial/Disturbed	1.8	1.6	1.8	2.0	2.2	1.9	–	2.3	2.1	2.1	2.0	2.2	2.1	2.3
	Interglacial/Disturbed	0.19	0.17	0.18	0.18	0.20	0.19	–	0.18	0.18	0.17	0.18	0.19	0.20	0.21
	Disturbed /Glacial flour	1.5	1.5	1.4	1.4	1.5	1.4	–	1.4	1.3	1.3	1.4	1.3	1.3	1.2
	Glacial flour/Accreted I	2	2	2	3	6	8	–	6	8	8	9	9	9	9
	Accreted I/Accreted II	>21	>18	>30	>19	>13	>1	–	>9	>28	>15	>19	>5	>16	>4
Maximum (pg g^{-1})	Interglacial stage	2	5	1	2	0.4	0.1	<0.6	0.05	0.3	0.06	0.2	0.02	0.1	0.02
	Glacial stage	23	56	7	25	5.6	1.2	<7	0.7	4	0.8	2.1	0.30	1.9	0.24
	Disturbed	11	29	2.9	10	2.1	0.5	<1.9	0.27	1.5	0.28	0.7	0.10	0.7	0.09
	Glacial flour	11	26	2.7	9	1.8	0.4	<1.3	0.21	1.2	0.22	0.6	0.08	0.5	0.07
	Accreted I	8	24	1.6	5	0.9	0.2	<1.4	0.10	0.6	0.09	0.25	0.03	0.2	0.02
	Accreted II	<2	<5	<0.5	<2	<0.2	<0.03	<0.2	<0.03	<0.2	<0.03	<0.08	<0.01	<0.06	<0.003
Minimum (pg g^{-1})	Interglacial stage	0.32	0.8	0.09	0.32	0.09	0.02	<0.05	0.007	0.05	0.01	0.02	0.005	0.03	0.0035
	Glacial stage	2.4	5.4	0.6	2.1	0.5	0.09	<0.6	0.05	0.25	0.05	0.12	0.016	0.09	0.015
	Disturbed	1.7	4.3	0.5	1.6	0.3	0.1	<0.2	0.05	0.25	0.05	0.12	0.017	0.10	0.014
	Glacial flour	0.5	1.8	0.2	0.6	0.1	0.03	<0.1	0.020	0.13	0.03	0.07	0.009	0.06	0.006
	Accreted I	0.05	0.3	0.002	0.01	<0.01	<0.004	<0.03	<0.001	<0.003	<0.0003	<0.001	<0.001	<0.002	<0.0004
	Accreted II	<0.04	<0.1	<0.006	<0.01	<0.01	<0.03	<0.03	<0.002	<0.003	<0.001	<0.002	<0.001	<0.002	<0.001
Maximum/Minimum	Interglacial stage	6	6	6	5	4	4	–	7	6	6	7	4	5	6
	Glacial stage	10	10	11	12	12	13	–	16	16	17	18	19	21	17
	Disturbed	6	7	6	6	6	6	–	6	6	6	6	6	7	6
	Glacial flour	21	14	15	15	18	13	–	11	9	9	8	9	9	12
	Accreted I	157	95	792	379	>86	>48	–	>114	>193	>310	>254	>61	>114	>58
Median crustal enrichment factor (AI)	Interglacial stage	1.8	2.2	2.2	1.8	2.4	2.2	<3.8	2.2	2.0	1.8	1.8	2.1	1.9	1.5
	Glacial stage	3.2	3.8	3.9	3.6	4.1	3.6	<7.2	4.3	4.1	3.7	3.8	3.7	3.6	2.7
	Disturbed	1.3	1.7	1.6	1.4	1.5	1.4	<1.8	1.6	1.5	1.4	1.4	1.3	1.2	0.9
	Glacial flour	1.1	1.4	1.4	1.2	1.3	1.2	<1.3	1.3	1.3	1.2	1.2	1.1	1.1	0.8
	Accreted I	8.6	13.0	9.6	6.2	6.9	7.1	<3.6	5.1	5.0	5.7	3.7	5.1	3.2	4.0
	Accreted II	–	–	–	–	–	–	–	–	–	–	–	–	–	–

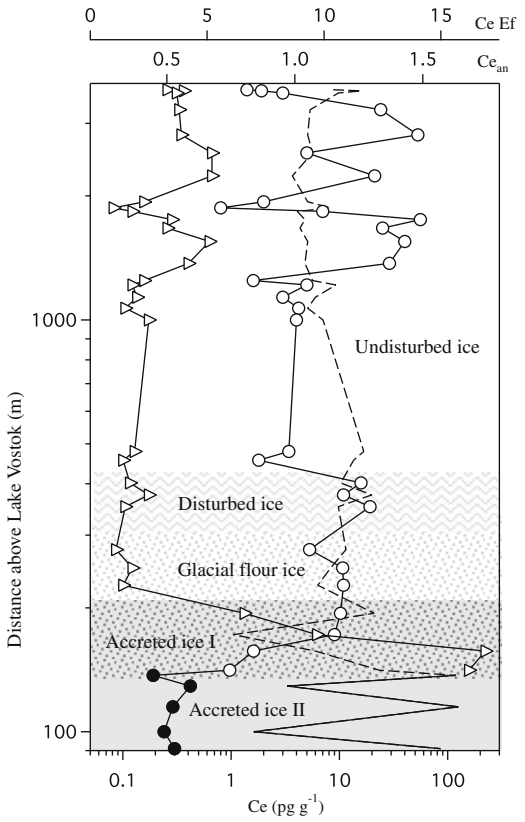

Fig. 4. Ce behavior in the Vostok ice core presented in terms of median Ce concentration (open circles; filled circles indicate the upper limits of concentration), Ce enrichment factor (defined as $EF_c = \{[Ce]_{ice}/[Al]_{ice}\}/\{[Ce]_{crust}/[Al]_{crust}\}$, where $[Ce]_{crust}$ and $[Al]_{crust}$ are the average Ce and Al concentrations in the upper continental crust (Wedepohl, 1995); open triangles) and Ce anomaly (Ce_{an} dashed line; the solid line indicates Ce_{an} obtained by upper limits of concentration). Owing to the very high correlations between Ce and the other REE, Ce is broadly representative of the relative variations in all REE concentrations. The highest REE concentrations were found in glacial stage ice and the lowest concentrations were in Accreted Ice Type II. Note that disturbed and glacial flour ice sections show intermediate concentrations when compared to the range of the undisturbed ice values. Relatively high Ce EF_c found in Accreted Ice Type I are characteristic of the LREE only. Regarding Ce_{an}, accreted ice sections tend to show much higher Ce_{an} variability than glacier ice.

of the main general variations in REE concentrations along the Vostok ice core.

Median REE levels in disturbed ice ($Ce = 16$ pg g^{-1}; $Lu = 0.05$ pg g^{-1}) are lower, by a factor of ~2, than in glacial stage ice but higher, by a factor of ~5, than in interglacial stage ice, in agreement with dust variability (Simoes et al., 2002). As the glacial climate regime (high dust fallout) largely dominates by time over the interglacial regime (low dust fallout) (Delmonte et al., 2004a), this is also consistent with data obtained from indistinguishable glacial/interglacial stage ice layers in the disturbed zone. Disturbed and glacial flour ice show median concentrations of the same order (16–11 pg g^{-1} for Ce and 0.05–0.04 pg g^{-1} for Lu, respectively). Nearly identical crustal enrichment factors and ratios of the median REE concentrations (Table 2) point to a similar dust composition in disturbed and glacial flour ice. If we assume that the upper disturbed layers are not remarkably influenced by bedrock particles, this observation suggests that the dust mass contribution from the bedrock to the glacial flour ice is minor relative to the aeolian input.

Interestingly, glacial flour ice median REE concentrations are higher, by a factor of ~2 for LREE and by a factor of ~9 for HREE, than in AC_1. As detailed in the following comparison of REE crustal patterns, this indicates an enrichment of LREE in AC_1. Finally, AC_1 shows median REE concentration values that are, in general, at least one order of magnitude higher than in AC_2. Previous studies reported that Holocene Antarctic ice and snow show the lowest trace element content in any natural matrix (Planchon et al., 2002; Vallelonga et al., 2002b). However, AC_2 retrieved from Lake Vostok displays even lower levels that constitute the lowest REE concentrations ever reported not only for snow and ice, but for all natural waters (see Table 3 for a review).

Due to the large observed heterogeneity in REE concentrations, maximum REE concentrations in AC_1 ($Ce = 24$ pg g^{-1}; $Lu = 0.02$ pg g^{-1}) are comparable to maximum concentrations in disturbed ice ($Ce = 29$ pg g^{-1}; $Lu = 0.09$ pg g^{-1}) and in glacial flour ice ($Ce = 26$ pg g^{-1}; $Lu = 0.07$ pg g^{-1}). In contrast, minimum REE concentrations in AC_1 ($Ce = 0.3$ pg g^{-1}; $Lu < 0.0004$ pg g^{-1}) are lower than minimum concentrations found in disturbed ice ($Ce = 4.3$ pg g^{-1}; $Lu = 0.014$ pg g^{-1}) and in glacial flour ice ($Ce = 1.8$ pg g^{-1}; $Lu = 0.006$ pg g^{-1}). The range of REE levels observed in AC_1 is at least one order of magnitude larger than in disturbed and glacial flour ice, congruent with an enrichment of REE carrying particles in aggregates dispersed within AC_1. We suggest that this large range might be due to a solid-phase exclusion process occurring within AC_1 during its formation, consistent with the idea of host water refreezing in separated pockets of frazil ice (Jouzel et al., 1999).

3.3. Ce anomaly

We calculate the Ce anomaly as:

$$Ce_{an} = \frac{2 * [Ce]}{*[La] + *[Pr]}$$

where the asterisk indicates the normalized concentration to the crustal mean (Wedepohl, 1995). In general Ce_{an} is positive (>1) in most of the Vostok ice sections (Fig. 4). Average Ce_{an} is 1.04 ($\sigma = 0.02$) in glacial stage ice, 1.15 ($\sigma = 0.08$) in interglacial stage ice, 1.22 ($\sigma = 0.07$) in disturbed ice, 1.14 ($\sigma = 0.05$) in glacial flour ice, 1.12 ($\sigma = 0.26$) in AC_1 and 1.33 ($\sigma = 0.35$) in AC_2. Interestingly, a small deviation of Ce_{an} during glacial periods (1.04 ± 0.02) points to a crustal-like composition of the aeolian particles.

Ce_{an} shows marked glacial/interglacial variation that may indicate contributions of aeolian dust from different sources during different climatic periods, as suggested by previous work (Delmonte et al., 2004a; Siggaard-Andersen et al., 2007; Ruth et al., 2008). A large variation in Ce_{an}

Table 3
REE concentrations (pg g^{-1}) determined in natural waters

	Reference	Value	La	Ce	Pr	Nd	Sm	Eu	Gd	Tb	Dy	Ho	Er	Tm	Yb	Lu	∑ REE
Accreted ice I from Lake Vostok	This study	Median	2.4	5.3	0.5	1.4	0.13	0.026	<0.14	0.02	0.08	0.02	0.04	0.005	0.03	0.004	9.9
Accreted ice II from Lake Vostok	This study	Median	<0.1	<0.3	<0.02	<0.07	<0.01	<0.03	<0.03	<0.002	<0.003	<0.001	<0.002	<0.001	<0.002	<0.001	<0.6
Seawater																	
North Pacific	Piepgras and Jacobsen, 1992; Zhang et al., 1994	Single value	5.6	0.7	0.7	3.3	0.57	0.17	0.9	0.17	1.1	0.36	1.2	0.2	1.2	0.230	16
Southern Ocean	Nozaki and Sotto Alibo, 2003	Minimum	0.46	0.36	0.10	0.59	0.14	0.05	0.24	0.04	0.14	0.12	0.36	0.06	0.31	0.05	3
Indian Ocean	Amakawa et al., 2000	Minimum	0.21	—	0.06	0.41	0.19	0.06	0.18	0.06	0.16	0.12	0.35	0.05	0.28	0.04	2
Lakes																	
Vanda (Antarctica)	De Carlo and Green, 2002	Minimum	9445	5884	1550	6056	—	—	—	—	—	—	—	—	—	—	22936
Mono Lake (California)	Johannesson and Lyons, 1994	Minimum	10	64	10	64	26	5	48	13	47	35	139	24	166	26	677
Navasha (Kenya)	Ojiambo et al., 2003	Single value	113	193	21	82	16	3	18	3	6	3	9	1	8	1	478
Streams/Rivers																	
Vosges (France)	Aubert et al., 2002	Single value	27	73	14	85	39	7	50	8	47	8	23	3	26	4	413
Sierra Pampeanas (Argentina)	Garcia et al., 2007	Minimum	16	35	5	21	5	1	4	—	2	2	3	—	3		97
Idaho (USA)	Nelson et al., 2003	Single value	171	313	41	181	37	9	42	6	4	8	30	5	46	10	903
Springs																	
Sardinia (Italy)	Biddau et al., 2002	Single value	19	17	14	20	17	10	14	7	8	10	9	7	12	5	169
Vosges (France)	Aubert et al., 2002	Single value	51	174	33	195	95	17	152	27	145	23	57	7	50	7	1033
Idaho (USA)	Nelson et al., 2003	Single value	30	63	11	48	15	3	15	3	17	3	10	2	11	2	233
Groundwater																	
Coffer (Nevada)	Johannesson et al., 1996	Single value	0.6	—	0.2	0.7		0.05	0.1	0.02	0.04	0.03	0.1	0.02	0.1	0.02	1.9
Navasha (Kenya)	Ojiambo et al., 2003	Single value	13	30	4	16	9	0.5	6	1	3	3	10	2	11	2	110
Saskathenwan (Canada)	Johannesson and Hendry, 2000	Minimum	2	6	1	2	1	0.3	1	0.3	1	0.5	3	1	4	1	23
Precipitation																	
Glacier, Vostok ice (Antarctica)	This study	Median	2.4	5.4	0.6	2.1	0.5	0.1	0.6	0.1	0.3	0.1	0.2	0.02	0.1	0.02	12
Rainwater, Vosges (France)	Aubert et al., 2002	Single value	2	1	0.2	1	1	0.2	1	0.2	1	0	1	0.2	1	0.2	10
Snow, Alps (France)	Aubert et al., 2002	Single value	3	16	2	11	6	2	8	1	8	1	4	0.4	3	0.3	66

appears in AC_1 where we can observe the maximum Ce_{an} (1.33) and the most negative Ce_{an} (0.76), similar to typical Ce_{an} found in saline marine waters (Alibo and Nozaki, 1999). A similar large variability is apparent in AC_2 (if REE concentrations in AC_2 are assumed to be reliable; see discussion in Section 2.2). These large Ce_{an} variations are difficult to interpret and might point to changes in the geochemistry of the lake as well as to undetermined chemical fractionation processes.

Finally, Ce_{an} in disturbed ice (1.22 ± 0.07) and glacial flour ice sections (1.14 ± 0.05) show roughly similar values. Because of the rather high REE concentrations in this basal ice, we believe that interglacial stage ice, although it displays similar Ce_{an} values (1.15 ± 0.08), is unlikely to have substantially influenced the geochemical composition of these sections. In contrast, as glacial stage dust fallout largely dominated by time over the climatic cycles (showing $Ce_{an} = 1.04 \pm 0.02$), its signature should be reflected in the basal ice. Thus, clearly distinct Ce_{an} values observed in the basal ice may indicate the presence of additional insoluble impurities originating from the bedrock.

3.4. REE normalized patterns

We now consider the patterns of the logarithms of the REE concentrations normalized to the average crustal composition (Wedepohl, 1995) (Fig. 5) and we report the LREE, MREE and HREE relative crustal enrichments (e.g., mean $LREE_{cr}$/mean $MREE_{cr}$) within the text. Some of the interglacial stage ice sections, in particular those from the Holocene (127 m) and MIS 11 (3271 and 3294 m), show enrichment in LREE when compared to MREE (31%, 50% and 34%) and HREE (49%, 94% and 44%, respectively). Also, the sample enriched in LREE at 1206 m (17% on MREE and 71% on HREE) is from a relatively mild stage, as deduced by the corresponding stable isotope ratio ($\delta D = -460‰$) which is taken as a proxy of past Vostok air temperature (Petit et al., 1999). The LREE enrichment found in these few Vostok interglacial stage samples is probably typical of East Antarctic ice during warm periods as such enrichment is also observed in Holocene ice from the EPICA Dome C core (Gabrielli et al., 2009).

Nevertheless, most of the undisturbed glacial stage ice sections show a crustal-like signature with a rather flat pattern and only a slight enrichment in MREE (on average 9% on LREE and 17% on HREE) during glacial periods. This is in excellent agreement with REE patterns previously reported for filtered dust from glacial stage sections of the Vostok and Dome C cores (Basile et al., 1997). These REE patterns were interpreted as diagnostic of aeolian dust originating from Patagonia. We note that these patterns are also consistent with a homogeneous mix of continental dust sources possibly producing a crustal-like signature.

Remarkably, AC_1 sections show a clear enrichment in LREE (in median 94% on MREE and 204% on HREE) that is independent of concentration level. For instance, the ice samples extracted from the section at 3593 m show highly variable REE concentrations (in a range of 1–20 pg g^{-1} for Ce) but consistently strong LREE enrichment (90–1800% on MREE and 330–2300% on HREE) (Fig. 3). Thus, as possibly evidenced by large variations in Ce_{an}, REE crustal patterns also indicate a distinct geochemical signature of undisturbed glacial stage ice (crustal-like composition) with respect to AC_1 (LREE enrichment).

If we compare the three sections from the disturbed layers, the one at 3374 m shows an enrichment in LREE (21% on MREE and 48% on HREE) and the other two (3348 and 3398 m) show a crustal-like REE signature. Similarly, two of the three glacial flour ice sections (3473 and 3523 m) show a crustal-like signature while the section at 3500 m produced only one aliquot enriched in LREE (26% on MREE and 64% on HREE) (Fig. 3). The occasional LREE enrichment in disturbed ice and glacial flour ice is not likely due to the presence of interglacial stage dust. In fact, high REE concentrations and rather low δD values (−465‰) in the 3374 and 3473 m ice sections do not support such a hypothesis. REE patterns in disturbed and glacial flour ice may instead indicate the prevalence of aeolian glacial stage dust and the sparse occurrence of a few bedrock particles/aggregates. This would be consistent with the heterogeneous REE concentrations observed within the basal ice sections, and may suggest that material from the bedrock could have been entrained further up-core in the disturbed ice than previously thought (Simoes et al., 2002). Further work utilizing Sr and Nd isotopes would be useful testing this emerging hypothesis.

3.5. Nature of the insoluble particles in AC_1

The two possible sources of insoluble particles observed in AC_1 are eroded detritus (from the bedrock itself and associated sedimentary deposits) and aeolian dust, the majority of which was likely deposited on the ice sheet during glacial stages and subsequently introduced to the lake by melting of the overlying glacier ice. As previously noted, the most distinctive feature observed in AC_1 is a marked LREE enrichment. If this enrichment is geochemically characteristic of the bedrock and is not the result of a chemical fractionation occurring in Lake Vostok water (see below), it would point to a direct contribution from a felsic substrate, consistent with an old Precambrian/Paleozoic basement lying below the ice (Delmonte et al., 2004b). We also note that this LREE enrichment might support the absence of high enthalpy processes from the mantle influencing the bedrock (Jean-Baptiste et al., 2001). In fact, as mantle material is depleted in LREE with regards to chemically-evolved, upper-crustal rocks of the continents, such processes likely would have resulted in a chondritic-like LREE depletion in the lake water and, by extension, the overlying ice.

Insoluble particles are likely introduced to Lake Vostok at its northern end where melting of the overlying ice sheet occurs and entrained aeolian dust can subsequently be released (Royston-Bishop et al., 2005). In general, atmospheric precipitation is considered significant in controlling REE concentration in watersheds (Garcia et al., 2007). It was demonstrated that between 50% and 90% of La and Sm in precipitation occurs in the particulate form (Heaton et al., 1990). A similar observation was made for tropical African rainwater (75%) (Freydier et al., 1998). It is therefore possible that REE

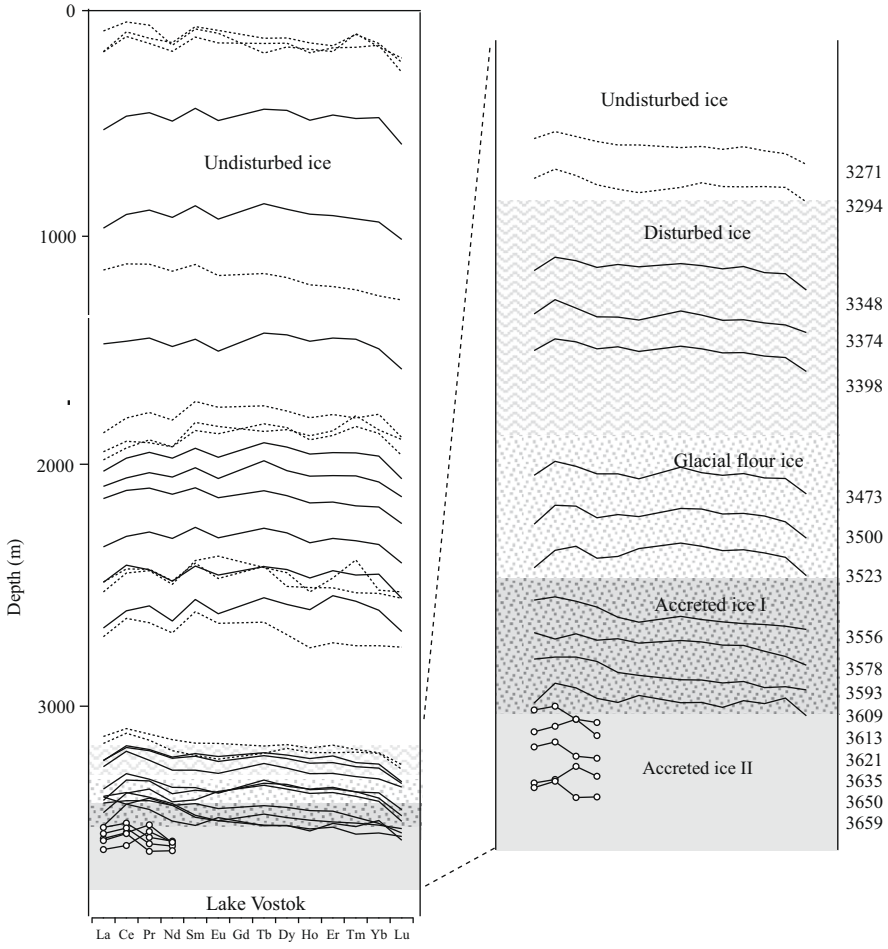

Fig. 5. Logarithm of the crustal-normalized median REE concentrations as a function of ice depth and type of ice. The panel on the right is expanded to highlight the deepest part of the Vostok ice core. Each REE pattern is equally constrained between its maximum and minimum values. Open circles indicate patterns obtained by upper limits of concentration. Dotted REE patterns are representative of mild glacial stage and interglacial periods ($\delta D > -460‰$). As Gd is biased by instrumental spectral interferences, its normalized concentration is only graphically interpolated through Eu and Tb. We note that a rather flat and crustal-like REE pattern is characteristic of the undisturbed ice sections during glacial stages and a LREE enrichment can be observed in a few interglacial stage ice sections. A LREE enrichment is more apparent in Accreted Ice Type I.

transported by particles of aeolian origin can influence the REE content of Lake Vostok, and thus of AC_1.

Interestingly, MREE and HREE in AC_1 are correlated with several trace elements determined in the same samples ($N = 35$), such as Al and Mn ($R^2 = \sim 0.7$) as well as Fe, Co and Rb ($R^2 = \sim 0.6$). In addition, MREE and HREE in AC_1 show crustal enrichment factors (EF_c; Al is taken as a crustal reference; see caption of Fig. 4) that are always close to unity. This information reinforces the idea that MREE and HREE in AC_1 are linked to crustal particles. In contrast, LREE in AC_1 are less correlated with Al, Mn, Fe, Co and Rb ($R^2 = \sim 0.3$ to ~ 0.4) and show higher median EF_c (~ 10; see Table 2) with sparse, very high EF_c (up to ~ 500; see Electronic annex 1), likely due to additional input from a different source and/or to LREE sorption/de-sorption processes occurring in Lake Vostok water. The situation is different when considering glacier ice as REE show uniformly high correlations ($R^2 > 0.9$) with Al, Mn, Fe, Co and Rb and EF_c generally close to unity. An exception occurs for Mn and Co which shows very low correlations with REE in disturbed ice. Overall, these correlations and EF_c suggest that MREE/HREE and LREE in AC_1 are from different sources. One possibility is that particles of aeolian origin represent the main input of MREE and HREE to AC_1 while a felsic bedrock contribution is responsible for the LREE enrichments. Alternatively, as discussed below, a chemical fractionation of REE, occurring within Lake Vostok and AC_1, could result in LREE enrichment.

If our data indicate that the large and complex aggregates observed in AC_1 contain aeolian particles and bedrock fragments, they would be consistent with the transport mechanism suggested by Royston-Bishop et al. (2005). This work concluded that particles of aeolian origin, entering the lake from melting glacier ice at its northern end, could be circulated before being entrapped in the accreted ice above the southern end. Interestingly, these authors found evidence of an additional source of very angular material,

possibly resulting from glacial erosion of the bedrock upstream of the lake that would also be consistent with an additional input of felsic particles from the bedrock.

3.6. REE geochemistry of Lake Vostok: possible scenarios

One must remain cautious in linking REE concentrations found in the accreted ice to the supposed REE content of Lake Vostok water, which has yet to be sampled directly. Accreted ice formation is complex and its mechanisms are not yet clearly understood. Refreezing can lead to strong separation of insoluble particles (Royston-Bishop et al., 2005) and soluble species by means of exclusion and concentration processes (Killawee et al., 1998). Such physical partitioning may be a particularly important consideration for the transparent, clean ice of AC_2 due to its extremely slow rate of formation ($\sim$10 mm y^{-1}) (Petit, 2005; Petit et al., 2005).

The heterogeneous REE distribution and the large range of concentrations in AC_1 may imply that REE exclusion and concentration processes have been confined to very small (several cm or less) spatial scale, consistent with the occurrence of frazil ice pockets (Jouzel et al., 1999). This could be valid for the insoluble and also for the soluble REE species (REE^{3+}) in AC_1 as most of the major ions are linked to visible aggregate content (De Angelis et al., 2004) and brine inclusions at the sub-mm scale (De Angelis et al., 2005). Thus, despite the fact that adjacent AC_1 ice volumes were enriched/depleted in REE, it seems reasonable to assume that median AC_1 REE concentrations could be broadly indicative of the REE content of Lake Vostok water, regardless of the cm-scale fractionation processes. As no direct chemical information about Lake Vostok is yet available, we recognize the speculative character of this assertion. However, following this approach, AC_1 might provide an initial tentative constraint on the REE geochemistry of Lake Vostok water.

Of particular note are the extremely low REE concentrations in AC_1. As these seem to be driven by insoluble particle content, REE concentrations linked to soluble species must be even lower. Given that Lake Vostok has likely been in direct and prolonged contact with the bedrock, the long residence time ($\sim$80 kyr) (Petit, 2005; Petit et al., 2005) should have produced an appreciable REE dissolution via hydrolysis at the bedrock/lake interface. Thus, one would expect REE concentrations in Lake Vostok to fall within the range observed in natural waters in contact with bedrock. However, the total REE median content ($\sum$REE) found in AC_1 (9.9 pg g^{-1}) is at the lower end of $\sum$REE found in seawater (2–30 pg g^{-1}) and is lower than that in lakes (100–40,000 pg g^{-1}), rivers (100–1000 pg g^{-1}), groundwater (10–100 pg g^{-1}) and even atmospheric precipitation (10–50 pg g^{-1}; see Table 3 for a review). We also note that $\sum$REE in AC_2 is much lower (<0.6 pg g^{-1}) than that in any natural water on Earth, strongly supporting the idea that physical partitioning processes must have occurred during the formation of AC_2.

Can the soluble REE content of Lake Vostok be effectively as low as that of AC_1? pH and salinity play a fundamental role in explaining the aquatic geochemistry of the soluble REE fraction. In general, REE should be more efficiently released from the geological substrate if pH is lower than 7. In contrast, REE should be mostly removed from solution under alkaline conditions (Garcia et al., 2007). Although we have no information about the lake's HCO_3^- and CO_3^{2-} content (important for controlling the pH in natural waters), the significant salt content in Vostok accreted ice may indicate that pH is neutral or slightly alkaline (De Angelis et al., 2004). Under these conditions the concentration of the soluble REE fraction in Lake Vostok water should be the lowest in the pH spectra (Johannesson and Burdige, 2007). This might explain, in part, the low REE content found in AC_1. However, as such low REE concentrations have never been observed in even slightly alkaline fresh waters, it is likely that net physical exclusion processes of dissolved species between AC_1 and Lake Vostok have also played a significant role.

In neutral or slightly alkaline conditions, such as those likely present in Lake Vostok, carbonate complexes dominate (>99%) the soluble REE fraction (Johannesson et al., 1996). In this scenario, the soluble REE fraction dissolved in Lake Vostok should show a HREE enrichment due to the preferential complexation of HREE with carbonates, hydroxide and fluoride (Nelson et al., 2003). Such an enrichment is not observed in AC_1. Assuming that that there is no difference in the partitioning of complexed and free REE at the ice/water interface, this would lend support to the idea that REE in AC_1 primarily reflects the geochemistry of the insoluble particle content.

Slightly alkaline conditions (pH = 7–8) act to stabilize dissolved HREE relative to LREE. The observed LREE enrichment in AC_1 could result from the greater affinity of dissolved positively charged $LREECO_3^+$ species for clay minerals (Johannesson and Hendry, 2000) suspended in the lake. These are relatively abundant in East Antarctic glacial stage dust in Vostok glacier ice (Delmonte, 2003) and should have been released into the lake (Royston-Bishop et al., 2005). Indeed relatively large amounts of clay minerals were found in AC_1 (Leitchenkov et al., 2007). In this case, the REE patterns would reflect a crustal-like terrestrial composition (possibly derived from the glacial stage aeolian dust) enriched in dissolved LREE via hydrolysis of the substrate.

In natural waters, REE^{+3} is characterized by a high charge/ionic radius ratio, which helps sorption onto suspended colloidal materials such as Fe and Mn oxyhydroxides and organic matter (German et al., 1990). For circum-neutral pH waters, modeling work predicts that REE will predominantly occur in solution as organic complexes (Tang and Johannesson, 2003). However, in that study no remarkable REE fractionation was simulated, ruling out the possibility of a link between the observed LREE enrichment in AC_1 and the presence of organic material in Lake Vostok. This is consistent with the very low levels of dissolved organic carbon (DOC) in accreted ice (Bulat et al., 2004).

Finally, we note that REE data are unlikely to offer insight into the suggested hydrothermal influence on Lake Vostok water (Bulat et al., 2004). Non-acidic contributions from hydrothermal sources would likely add only a minor amount of soluble REE and would be overwhelmed by the particulate fraction which dominates the REE content in AC_1.

4. CONCLUSIONS

Despite the presence of millimeter-sized soft terrigenous aggregates, AC_1 shows REE concentrations that are generally lower than those found in natural fresh waters and the deeper, transparent AC_2 shows concentrations that are even lower than in depleted seawater. Ultra-low REE concentrations in AC_1 and AC_2 are likely a result of phase exclusion processes, which partition particles and dissolved species between the ice and the water during refreezing.

We explain the observed heterogeneous spatial distribution of REE in AC_1 as resulting from enrichment of REE-carrying insoluble particles within the observed millimeter-sized aggregates, possibly due to an additional cm-scale solid phase exclusion process occurring within AC_1 during its formation. LREE enrichment suggests that these particles may have originated from a felsic basement. Alternatively, this LREE enrichment may reflect the preferential affinity of LREE (dissolved from the basement via hydrolysis) for clay particles of aeolian origin suspended in Lake Vostok.

Interestingly, REE patterns observed in the undisturbed ice layers are consistent with the presence of a well-homogenized mix of continental dust producing a crustal-like signature. These particles were transported to Antarctica primarily during past glacial stages and influence the geochemistry of the disturbed ice, glacial flour ice, and possibly that of the accreted ice and Lake Vostok water. However, these indirect geochemical observations on Lake Vostok water obtained from analysis of the accreted ice will be confirmed or disproved only when water samples are collected directly from the lake. This will be possible only by using clean techniques that avoid contamination from the drilling fluid.

ACKNOWLEDGMENTS

This work was supported in Italy by a Marie Curie Fellowship of the European Community (contract HPMF-CT-2002-01772) and by ENEA as part of the Antarctic National Research Program (under projects on Environmental Contamination and Glaciology). In France, it was supported by the Institut National des Sciences de l'Univers and the University Joseph Fourier of Grenoble. This is contribution number 1382 of the Byrd Polar Research Center. We thank the editor Karen Johannesson, Eric De Carlo, two other anonymous reviewers, Berry Lyons, Ellen Mosley-Thompson, Aron Buffen and Martine De Angelis for useful comments that significantly improved this manuscript. F.P. acknowledges support from the Balzan prize awarded to Claude Lorius.

REFERENCES

Alibo D. S. and Nozaki Y. (1999) Rare earth elements in seawater: particle association, shale-normalization, and Ce oxidation. *Geochim. Cosmochim. Acta* **63**(3/4), 363–372.

Amakawa H., Sotto Alibo D. and Nozaki Y. (2000) Nd isotopic composition and REE pattern in the surface waters of the eastern Indian Ocean and its adjacent seas. *Geochim. Cosmochim. Acta* **64**(10), 1715–1727.

Aubert D., Stille P., Probst A., Gauthier-Lafaye F., Pourcelot L. and Del Nero M. (2002) Characterization and migration of atmospheric REE in soils and surface water. *Geochim. Cosmochim. Acta* **66**(19), 3339–3350.

Basile I., Grousset F. E., Revel M., Petit J. R., Biscaye P. E. and Barkov N. I. (1997) Patagonian origin of glacial dust deposited in East Antarctica (Vostok and Dome C) during glacial stages 2, 4 and 6. *Earth Planet. Sci. Lett.* **146**, 573–589.

Bell R. E., Studinger M. R., Tikku A. A., Clarke G. K., Gutner M. M. and Meertens C. (2002) Origin and fate of Lake Vostok water frozen to the base of the East Antarctic ice sheet. *Nature* **416**, 307–310.

Biddau R., Cidu R. and Frau F. (2002) Rare earth elements in waters from the albitite-bearing granodiorites of Central Sardinia, Italy. *Chemical Geology* **182**, 1–14.

Bulat S., Alekhina I., Blot M., Petit J. R., de Angelis M., Wagenbach D., Lipenkov V. Y., Vasilyeva L. P., Wloch D. M., Raynaud D. and Lukin V. V. (2004) DNA signature of thermophilic bacteria from the aged accretion ice of Lake Vostok, Antarctica: implications for searching for life in extreme icy environments. *Int. J. Astrobiol.* **3**, 1–12.

Bulat S., Alekhina I., Lipenkov V. Y., Barnola J. M., Wagenbach D., de Angelis M., Leitchenkov G., Marie D., Normand P., Petit J. R. (2008) Biogeochemical study of lake Vostok accretion ice: Russian French team science update. In *SCAR/IASC IPY Open Science Conference*, SSC RF AARI, pp. 332–333.

Candelone J. P., Hong S. and Boutron C. F. (1994) An improved method for decontaminating polar snow and ice cores for heavy metals analysis. *Anal. Chim. Acta* **299**, 9–16.

Christner B. C., Royston-Bishop G., Foreman C. M., Arnold B. R., Tranter M., Welch K. A., Lyons W. B., Tsapin A. I., Studinger M. R. and Priscu J. C. (2006) Limnological conditions in subglacial Lake Vostok, Antarctica. *Limnol. Ocean.* **51**(6), 2485–2501.

Dahl-Jensen D., Thorsteinsson T., Alley R. B. and Shoji H. (1997) Flow properties of the ice from the Greenland Ice Core Project ice core: the reason for folds? *J. Geophys. Res.* **102**(C12), 26831–26840.

De Angelis M., Morel C., Barnola J.M., Susini J. and Duval P. (2005) Brine micro-droplets and solid inclusions in accreted ice from Lake Vostok, (East Antarctica). *Geophys. Res. Lett.* **32**(L12501), doi:10.1029/2005GL022460..

De Angelis M., Petit J. R., Savarino J., Souchez R. and Thiemens M. H. (2004) Contributions of an ancient evaporitic-type reservoir to subglacial Lake Vostok chemistry. *Earth Planet. Sci. Lett.* **222**, 751–765.

De Carlo E. H. and Green W. J. (2002) Rare earth elements in the water column of Lake Vanda, McMurdo Dry Valleys, Antarctica. *Geochim. Cosmochim. Acta* **66**(8), 1323–1333.

Delmonte B. (2003) Quaternary variation and origin of continental dust in East Antarctica, Thesis, University Joseph Fourier

Delmonte B., Basile-Doelsch I., Petit J. R., Maggi V., Revel-Rolland M., Michard A., Jagoutz E. and Grousset F. E. (2004a) Comparing the Epica and Vostok dust records during the last 220, 000 years: stratigraphical correlation and provenance in glacial periods. *Earth Sci. Rev.* **66**, 63–87.

Delmonte B., Petit J. R., Basile-Doelsch I., Lipenkov V. Y. and Maggi V. (2004b) First characterization and dating of East Antarctic bedrock inclusions from subglacial Lake Vostok accreted ice. *Environ. Chem.* **1**, 90–94.

Freydier R., Dupré B. and Lacaux J. P. (1998) Precipitation chemistry in intertropical Africa. *Atmos. Environ.* **32**(4), 749–765.

Gabrielli P., Barbante C., Turetta C., Marteel A., Boutron C. F., Cozzi G., Cairns W., Ferrari C. and Cescon P. (2006a) Direct determination of rare earth elements at the sub picogram per gram level in Antarctic ice by ICP-SFMS using a desolvation system. *Anal. Chem.* **78**, 1883–1889.

Gabrielli P., Planchon F., Hong S., Lee K., Hur S. D., Barbante C., Ferrari C., Petit J. R., Lipenkov V. Y., Cescon P. and Boutron

C. F. (2005) Trace elements in Vostok Antarctic ice during the last four climatic cycles. *Earth Planet. Sci. Lett.* **234**(1–2), 249–259.

Gabrielli P., Plane J. M. C., Boutron C. F., Hong S., Cozzi G., Cescon P., Ferrari C., Crutzen P., Petit J. R., Lipenkov V. Y. and Barbante C. (2006b) A climatic control on the accretion of meteoric and super-chondritic iridium-platinum to the Antarctic ice cap. *Earth Planet. Sci. Lett.* **250**, 459–469.

Gabrielli P., Varga A., Barbante C., Boutron C. F., Cozzi G., Gaspari V., Planchon F., Cairns W., Hong S., Ferrari C. and Capodaglio G. (2004) Determination of Ir and Pt down to the sub-femtogram per gram level in polar ice by ICP-SFMS using preconcentration and a desolvation system. *J. Anal. Atom. Spectrom.* **19**, 831–837.

Gabrielli P., Wegner A., Petit J. R., Delmonte B., De Dekker P., Gaspari V., Fisher H., Ruth U., Kriews M., Boutron C. F., Cescon P. and Barbante C. (2009) A major glacial-interglacial change in aeolian dust composition as inferred from rare earth elements in Antarctic ice. *Quat. Sci. Rev.*, in press.

Garcia G. M., Lecomte K. L., Pasquini A. I., Formica S. M. and Depetris P. J. (2007) Sources of dissolved REE in mountainous streams draining granitic rocks, Sierra Pampeanas (Cordoba, Argentina). *Geochim. Cosmochim. Acta* **71**, 5355–5368.

German C. R., Klinkhammer G. P., Edmond J. M., Mitra A. and Elderfield H. (1990) Hydrothermal scavenging of rare-earth elements in the ocean. *Nature* **345**, 516–518.

Heaton R. W., Rahn K. A. and H.L.D. (1990) Determination of trace elements, including regional tracers, in Rhode Island precipitation. *Atmos. Environ.* **24A**(1), 147–153.

Henderson P. (1984) rare earth element geochemistry. In *Developments in Geochemistry*, vol. 2. Elsevier Science, pp. 510..

Hong S., Boutron C. F., Barbante C., Do Hur S., Lee K., Gabrielli P., Capodaglio G., Ferrari C., Petit J. R. and Lipenkov V. Y. (2005) Glacial-interglacial changes in the occurrence of Pb, Cd, Cu and Zn in Vostok Antarctic ice from 240 to 410 kyr BP. *J. Environ. Monitor.* **7**(12), 1326–1331.

Hong S., Boutron C. F., Gabrielli P., Barbante C., Ferrari C., Petit J. R., Lee K. and Lipenkov V. Y. (2004) Past natural changes in Cu, Zn and Cd in Vostok Antarctic ice dated back to the beginning of the next to last ice age. *Geophys. Res. Lett.* **31**. doi:10.1029/2004GL021075.

Jean-Baptiste P., Petit J. R., Lipenkov V. Y., Raynaud D. and Barkov N. (2001) Constraints on hydrothermal processes and water exchange in Lake Vostok from helium isotopes. *Nature* **411**, 460–462.

Johannesson K. H. and Burdige D. J. (2007) Balancing the global oceanic neodymium budget: evaluating the role of groundwater. *Earth Planet. Sci. Lett.* **253**, 129–142.

Johannesson K. H. and Hendry M. J. (2000) Rare earth element geochemistry of groundwaters from a thick till and clay rich aquitard sequence, Saskatchewan, Canada. *Geochim. Cosmochim. Acta* **64**(9), 1493–1509.

Johannesson K. H. and Lyons W. B. (1994) The rare earth element geochemistry of Mono Lake water and the importance of carbonate complexing. *Limnol. Ocean.* **39**(5), 1141–1154.

Johannesson K. H., Stetzenbach K. J., Hodge V. and Lyons W. B. (1996) Rare earth element complexation behavior in circumneutral pH groundwaters: assessing the role of carbonate and phosphate ions. *Earth Planet. Sci. Lett.* **139**, 305–319.

Jouzel J., Petit J. R., Souchez R., Barkov N. I., Lipenkov V. Y., Raynaud D., Stievenard M., Vassiliev N. I., Verbeke V. and Vimeux F. (1999) More than 200 m of Lake Ice above subglacial Lake Vostok, Antarctica. *Science* **286**, 2138–2141.

Kapitsa A. P., Ridley J. K., Robin G. d. Q., Siegert M. and Zotikov I. A. (1996) A large deep freshwater lake beneath the ice of central East Antarctica. *Nature* **381**, 684–686.

Killawee J. A., Fairchild I. J., Tison J. L., Janssens L. and Lorrain R. (1998) Segregation of solutes and gases in experimental freezing of dilute solutions: implications for natural glacial systems. *Geochim. Cosmochim. Acta* **62**(23/24), 3637–3655.

Lavire C., Normand P., Alekhina I., Bulat S., Prieur D., Birrien J.-L., Fournier P., Hanni C. and Petit J. R. (2006) Presence of Hydrogenophilus thermoluteolus DNA in accretion ice in the subglacial Lake Vostok, Antarctica, assessed using rrs, cbb and hox. *Environ. Microbiol.* **8**(12), 2106–2114.

Leitchenkov G., Belyatsky B.V., Rodionov N.V. and Sergeev S.A. (2007) Insights into the geology of the East Antarctic hinterland: a study of sediment inclusions from ice cores of the Lake Vostok borehole. In *Antarctica: A Keystone in a Changing World — Online Proceedings of the 10th ISAES* (eds. A. K. Cooper and C. R. Raymond), pp. 4.

Masolov V. N., Lukin V. V., Popov S., Popkov A. N., Sheremetiev A. N. and Kruglova U. A. (2008) Seabed relief of the subglacial Lake Vostok. In *SCAR/IASC IPY Open Science Conference*, SSC RF AARI.

Masolov V. N., Lukin V. V., Sheremetiev A. N. and Popov S. (2001) Geophysical investigations of the subglacial Lake Vostok, Antarctica. *Dokl. Akad. Nauk.* **379**, 680–685.

Nelson B. J., Wood S. A. and Osiensky J. L. (2003) Partitioning of REE between solution and particulate matter in natural waters: a filtration study. *J. Solid State Chem.* **171**, 51–56.

Nozaki Y. and Sotto Alibo D. (2003) Dissolved rare earth elements in the Southern Ocean, southwest of Australia: unique patterns compared to the South Atlantic data. *Geochem. J.* **37**, 47–62.

Ojiambo B. S., Lyons W. B., Welch K. A., Poreda R. J. and Johannesson K. H. (2003) Strontium isotopes and rare earth elements as tracers of groundwater-lake interactions, Lake Naivasha, Kenya. *App. Geochem.* **18**, 1789–1805.

Petit J. R. (2005) Geophysical, geochemical, glaciological and energy balance model constraints to the Lake Vostok. *Mater. Glyatsiol. issled.* **97**, 91–100.

Petit J. R., Alekhina I. and Bulat S. (2005) Lake Vostok, Antarctica: exploring a subglacial Lake and searching for life in an extreme environment. In *Lectures in Astrobiology*, vol. 1 (eds. M. Gargaud, B. Barbier, H. Martin and J. Reisse). Springer, pp. 227–288.

Petit J. R., Jouzel J., Raynaud D., Barkov N. I., Barnola J. M., Basile-Doelsch I., Bender M., Chappellaz J., Davis M., Delaygue G., Delmotte M., Kotlyakov V. M., Legrand M., Lipenkov V. Y., Lorius C., Pépin L., Ritz C., Saltzman E. and Stievenard M. (1999) Climate and atmospheric history of the past 420,000 years from the Vostok ice core, Antarctica. *Nature* **399**, 429–436.

Piepgras D. J. and Jacobsen B. (1992) The behavior of rare earth elements in seawater: precise determination of variations in the North Pacific water column. *Geochim. Cosmochim. Acta* **56**, 1851–1862.

Planchon F., Boutron C. F., Barbante C., Cozzi G., Gaspari V., Wolff E. W., Ferrari C. and Cescon P. (2002) Changes in heavy metals in Antarctic snow from Coats Land since the mid-19th to the late-20th century. *Earth Planet. Sci. Lett.* **200**, 207–222.

Royston-Bishop G., Priscu J. C., Tranter M., Christner B. C., Siegert M. and Lee V. (2005) Incorporation of particulates into accreted ice above subglacial Vostok lake. *Antarctica Ann. Glaciol.* **40**, 145–150.

Ruth U., Barbante C., Bigler M., Delmonte B., Fisher H., Gabrielli P., Gaspari V., Kaufmann P., Lambert F., Maggi V., Marino F., Petit J. R., Steffensen J. P., Udisti R., Wagenbach D., Wegner A. and Wolff E. W. (2008) Proxies and measurement techniques for mineral dust in Antarctic ice cores. *Environ. Sci. Technol.* **42**(15), 5675–5681.

Siegert M., Carter S., Tabacco I., Popov S. and Blankenship D. D. (2005) A revised inventory of Antarctic subglacial lakes. *Antarct. Sci.* **17**, 453–460.

Siegert M., Ellis-Evans J. C., Tranter M., Mayer C., Petit J. R., Salamatin A. and Priscu J. C. (2001) Physical, chemical and biological processes in Lake Vostok and other Antarctic subglacial lakes. *Nature* **414**, 603–609.

Siegert M., Kwok R., Mayer C. and Hubbard B. (2000) Water exchange between the subglacial Lake Vostok and the overlying ice sheet. *Nature* **403**, 643–646.

Siggaard-Andersen M. L., Gabrielli P., Steffensen J. P., Stromfeldt T., Barbante C., Boutron C. F., Fisher H. and Miller H. (2007) Soluble and insoluble lithium dust in the EPICA Dome C ice core – implications for changes of the East Antarctic dust provenance during the recent glacial – interglacial transition. *Earth Planet. Sci. Lett.* **258**, 32–43.

Simoes J. C., Petit J. R., Souchez R., Lipenkov V. Y., de Angelis M., Leibao L., Jouzel J. and Duval P. (2002) Evidence of glacial flour in the deepest 89 m of the Vostok ice core. *Ann. Glaciol.* **35**(1), 340–346, 7.

Souchez R., Jean-Baptiste P., Petit J. R., Lipenkov V. Y. and Jouzel J. (2002) What is the deepest part of the Vostok ice core telling us? *Earth Sci. Rev.* **60**, 131–146.

Souchez R., Petit J. R., Jouzel J., de Angelis M. and Tison J. L. (2003) Re-assessing Lake Vostok's behaviour from existing and new ice core data. *Earth Planet. Sci. Lett.* **217**, 163–170.

Studinger M. R., Bell R. E. and Tikku A. A. (2004) Estimating the depth and shape of subglacial Lake Vostok's water cavity from aero-gravity data. *Geophys. Res. Lett.* **31**(L12401). doi:10.1029/2004GL019801.

Tang J. and Johannesson K. H. (2003) Speciation of rare earth elements in natural terrestrial waters: assessing the role of dissolved organic matter from the modeling approach. *Geochim. Cosmochim. Acta* **67**(13), 2321–2339.

Vallelonga P., Van de Velde K., Candelone J. P., Ly C., Rosman K., Boutron C. F., Morgan V. I. and Mackey D. J. (2002a) Recent advances in measurment of Pb isotopes in polar ice and snow at sub-picogram per gram concentrations using thermal ionisation mass spectrometry. *Anal. Chim. Acta* **453**, 1–12.

Vallelonga P., Van de Velde K., Candelone J. P., Morgan V. I., Boutron C. F. and Rosman K. J. R. (2002b) The lead pollution history of Law Dome, Antarctica, from isotopic measurements on ice cores: 1500 AD to 1989 AD. *Earth Planet. Sci. Lett.* **204**(1–2), 291–306.

Wedepohl K. H. (1995) The composition of the continental crust. *Geochim. Cosmochim. Acta* **59**, 1217–1232.

Wingham D. J., Siegert M., Shepherd A. and Muir A. S. (2006) Rapid discharge connects Antarctic subglacial lakes. *Nature* **440**, 1033–1036.

Zhang J., Amakawa H. and Nozaki Y. (1994) The comparative behavior of yttrium and lanthanides in the sea water of the North Pacific. *Geophys. Res. Lett.* **21**, 2677–2680.

Associate editor: Karen Johannesson